Method to analyze the influence of switching behavior in hard switching half bridge topologies for traction application

Dominik Nehmer, Michael Gleissner, Lukas Bergmann, Mark-M. Bakran

UNIVERSITY OF BAYREUTH
DEPARTMENT OF MECHATRONICS
CENTER OF ENERGY TECHNOLOGY
Universitaetsstrasse 30
Bayreuth, Germany
Phone: +49 (0) 921 55-7822
Email: dominik.nehmer@uni-bayreuth.de
URL: http://www.mechatronik.uni-bayreuth.de

Acknowledgments

This paper was supported by the Federal Ministry for Economic Affairs and Climate Action based on a decision by the German Bundestag.

Federal Ministry
for Economic Affairs
and Climate Action

Keywords

≪Harmonics≫, ≪Silicon Carbide (SiC)≫, ≪Traction application≫, ≪Active front-end≫, ≪Voltage Source Converter (VSC)≫.

Abstract

The current harmonics feed back (interference current) of railway traction inverter towards the grid has to be limited. The goal of this paper is to present a method which allows to model harmonics caused by switching behavior and turn on delay. Since simulation is limited by numerical errors due to the step size of the numerical solvers and also takes much time, an analytical method is chosen.

Introduction

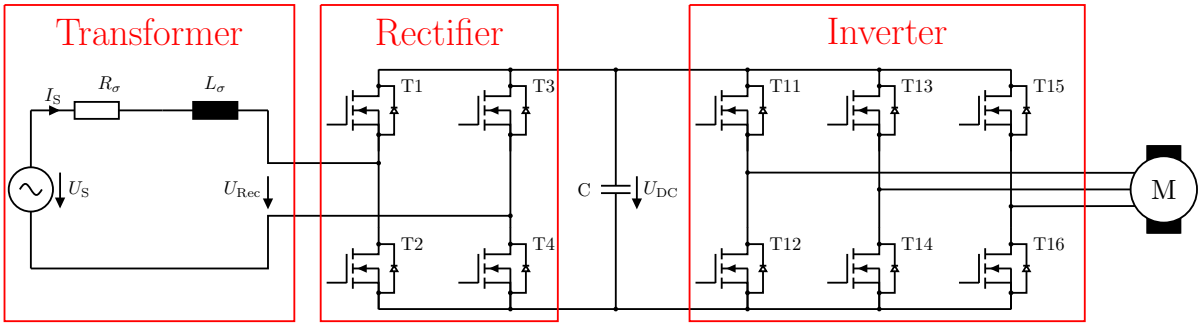

Fig. 1: Simplified circuit diagram of traction inverter

In Figure 1 a simplified circuit diagram of the traction inverter is shown. On the left side the secondary side of a transformer towards the grid is shown. L_σ represents the stray inductance of the transformer related to its secondary side and R_σ its resistance. The transistors T1 to T4 build up an active front end rectifier. Hence the converter is voltage based the intermediate circuit is a capacitor. The transistors

T11-T16 represent an inverter for the electrical machine M. The rectifier and the inverter are based on hard switching half bridges.

In the following the influence of the switching behavior on interference currents towards the grid is analyzed. First the calculation method of harmonics is presented. The next step is the modeling of the switching behavior. After this the method is compared to a simulation model approach. Then effects of the switching behavior on the harmonics based on the voltage spectrum are presented. The influence on the harmonics is compared for a Si IGBT and a SiC MOSFET power module. After this the current spectrum is calculated and the influence of the switching behavior on interference current is evaluated. Finally a conclusion and an outlook is given.

Method

Basic idea

In [1] and [2] an analytical method is presented by using Fourier analysis of carrier signal and superimposition of fundamental wave. For the calculation a Bessel function has to be solved. In [3] even the turn on delay is modeled based on this method. In the following a method is presented to model turn on delay $T_{\mathrm{d,o}}$ (to prevent half bridge short circuit) and switching times (equivalent voltage time area of commutation process). Therefore the switching behavior is modeled as a square area and an effective dead time with the same number of volt-seconds as described in [4]. Then the basic PWM signal is calculated using a synchronous sine triangular modulation. After this the switching angles of the PWM are applied by the switching dead times and turn on delay. Finally the Fourier spectrum is calculated.

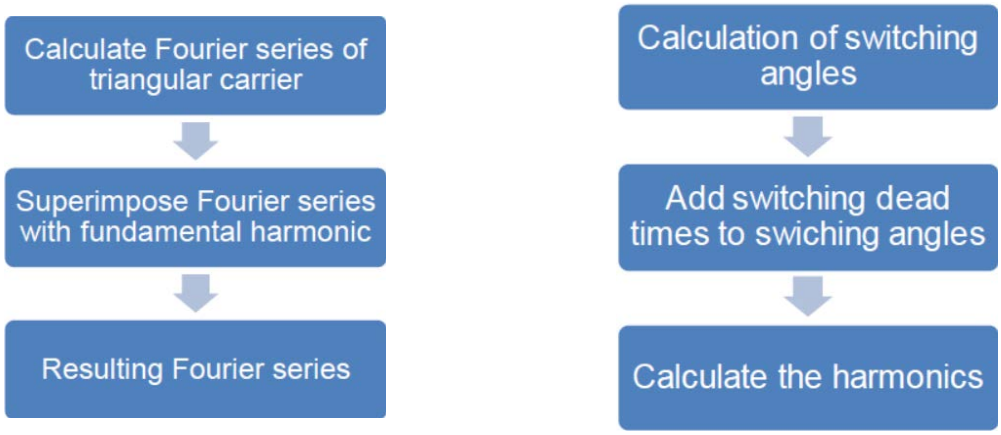

a) Method applied in [3]

b) Proposed method

Fig. 2: Current and proposed method to calculate Fourier coefficients

In Figure 2 b) the method for investigation of the influence on harmonics through switching characteristics is shown. In the first step the switching angles are calculated by using a synchronous sine triangular modulation. In the second step the switching angles are applied by the effective dead time of the switching process. In the last step the harmonics are calculated. Therefore the necessary equations are presented.

Calculation of the switching angles

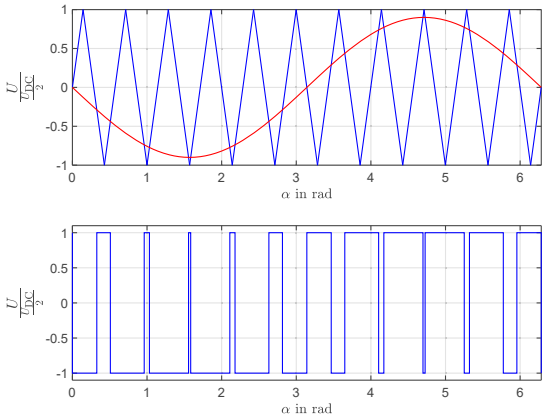

Fig. 3: Synchronous sine triangular modulation with resulting PWM signal

At the top of Figure 3 the fundamental wave (red) and the triangular carrier (blue) are shown. The modulation is a sine triangular modulation with natural sampling. This modulation and sampling scheme is chosen so that there are no harmonics between the carrier bands and the influence of the dead times can be identified clearly. At the bottom of the figure the resulting PWM signal is shown. The edges of the PWM signals are the switching angles without switching dead times.

Adding switching dead times to switching angles

Now the switching angles are added to the effective switching dead time. The dead time includes the turn on delay (to prevent a half bridge short circuit) and the effective voltage-time area of the commutation process. The effective voltage-time area of the commutation process can be expressed as a function of current, temperature and other parameters.

Calculation of the Fourier spectrum

$$\begin{aligned} u(\omega t) &= \sum_{k=1}^{\infty} \left(a_\mathrm{k} \cos(k\omega t) + b_\mathrm{k} \sin(k\omega t)\right) = \sum_{k=1}^{\infty} \left(\sqrt{a_\mathrm{k}^2 + b_\mathrm{k}^2} \cos(k\omega t) - \arctan\left(\frac{b_\mathrm{k}}{a_\mathrm{k}}\right)\right) \\ &= \sum_{k=1}^{\infty} \left(A_\mathrm{k} \cos(k\omega t - \varphi_\mathrm{k})\right) \end{aligned} \tag{1}$$

Equation 1 expresses the Fourier series of a periodic signal. The series can be described as a combination of sin and cos terms as given in the first row or as a cos term with amplitude and phase as given in the second row. The coefficients a_k and $b_\mathbf{k}$ have to be calculated. Therefore the following integral has to be solved sectionally:

$$\begin{aligned} a_\mathrm{k} &= \frac{1}{\pi} \int_{-\pi}^{\pi} \left(u(x) \cos(kx)\right) dx \\ &= \frac{1}{\pi} \left[\int_{-\pi}^{\alpha_1} \left(\frac{U_\mathrm{DC}}{2} \cos(kx)\right) dx - \int_{\alpha_1}^{\alpha_2} \left(\frac{U_\mathrm{DC}}{2} \cos(kx)\right) dx \pm \ldots - \int_{\alpha_l}^{\pi} \left(\frac{U_\mathrm{DC}}{2} \cos(kx)\right) dx\right] \\ &= \frac{U_\mathrm{DC}}{2k\pi} \left[\left(\sin(k\alpha_1)\right) - \sin(-k\pi) - \left(\sin(k\alpha_2)\right) - \sin(k\alpha_1) \pm \ldots - \left(\sin(k\pi)\right) - \sin(k\alpha_l)\right] \\ &= \frac{U_\mathrm{DC}}{k\pi} \left(\sum_{n=1}^{l} (-1)^{n+1} \sin(k\alpha_\mathrm{n})\right) \end{aligned} \tag{2}$$

The first line shows the definition of the coefficient a_k [5]. In the second line the integral is divided in parts. Each of the parts is separated by the switching angles. In each part the amplitude of the PWM

signal is $\pm\frac{U_{\mathrm{DC}}}{2}$. In the third line the integrals are solved. In the last line the coefficient a_k is expressed as a row of sin terms. The number of terms l equals the number of switching angles.

Now the Fourier spectrum can be calculated analytical. It is not necessary to calculate Bessel functions or to solve differential equations. Additionally, the switching angles can be varied separately, which allows to model switching dead time.

The coefficient b_k can be calculated accordingly and is given as follows:

$$b_{\mathrm{k}} = \frac{1}{\pi}\int_{-\pi}^{\pi}\left(u\left(x\right)\sin\left(kx\right)\right)\,dx = \frac{U_{\mathrm{DC}}}{k\pi}\left(\sum_{n=1}^{l}\left(-1\right)^{n+1}\cos\left(k\alpha_{\mathrm{n}}\right)\right) \tag{3}$$

Switching dead time

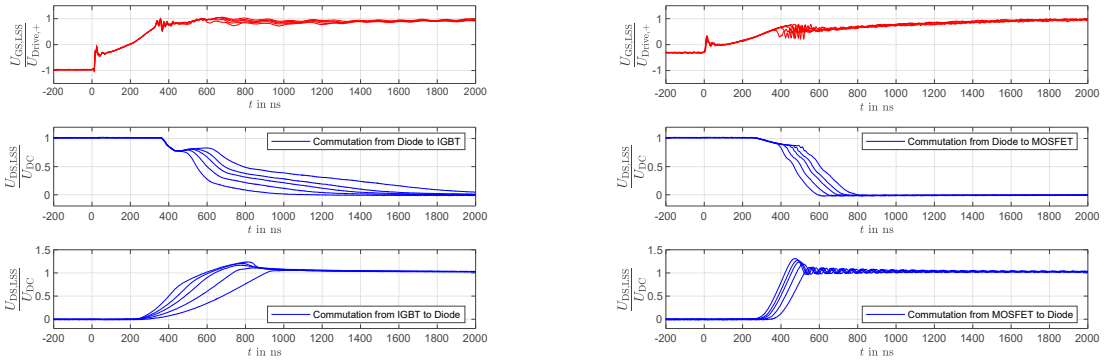

a) Mitsubishi CM600 Si-IGBT module

b) Comparable SiC-MOSFET module

Fig. 4: Voltage curves for different load currents of the traction inverter modules

In Figure 4 the voltage commutations for a Si-IGBT from $U_{\mathrm{DC+}}$ to $U_{\mathrm{DC-}}$ (middle) and from $U_{\mathrm{DC-}}$ to $U_{\mathrm{DC+}}$ (bottom) are shown. As already described in [4] the voltage slope can be modeled as a square wave and effective dead time. Both should have the same voltage-time area since it causes the additional harmonics.

Calculation of switching dead times

The effective switching-on time can be expressed as follows:

$$T_{\mathrm{on}} = \frac{1}{U_{\mathrm{DC}}}\int_{0}^{t_{\mathrm{switch,end}}}\left(u\left(t\right)\right)\,dt \tag{4}$$

Equivalent to the switching-on time the switching-off time is:

$$T_{\mathrm{off}} = \frac{1}{U_{\mathrm{DC}}}\int_{0}^{t_{\mathrm{switch,end}}}\left(U_{\mathrm{DC}} - u\left(t\right)\right)\,dt \tag{5}$$

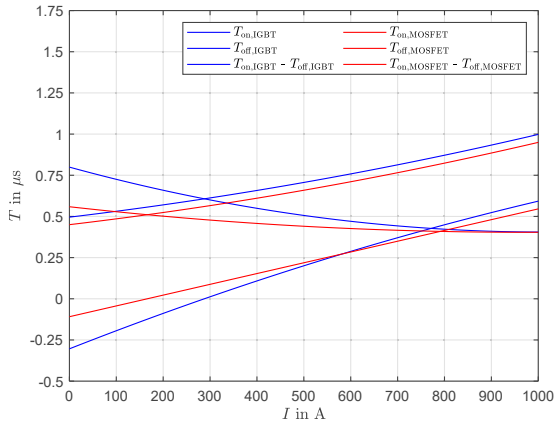

Fig. 5: Equivalent switching times of Si-IGBT and SiC-MOSFET as function of the current

In Figure 5 the switching times of Si IGBT an SiC MOSFET are shown. Both are moduls designed for railway traction application and have the same power rating. Also the difference between the turn-on and turn-off time is shown, since the difference causes an error of the voltage-time areas.

Switching angles with dead times

Table I: Relevant dead times for the different switching edges

	$U_{DC+} \rightarrow U_{DC-}$	$U_{DC-} \rightarrow U_{DC+}$
$I > 0$	T_{off}	$T_{on} + T_{d,on}$
$I < 0$	$T_{on} + T_{d,on}$	T_{off}

In Table I the relevant dead times for positive and negative voltage edges as well as positive and negative phase current are shown.

Comparison of methods

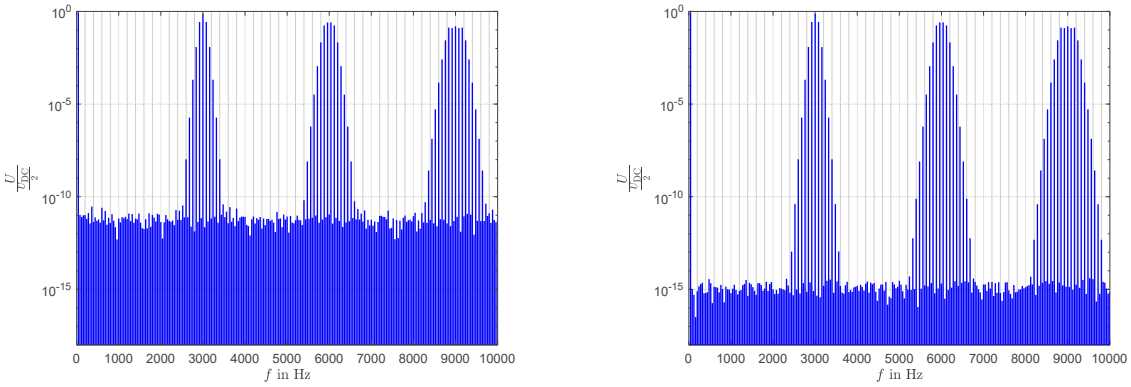

a) Simulation b) Analytical calculation

Fig. 6: Comparison of Fourier spectrum error precision of different methods ($f_1 = 200\,Hz$, $f_S = 3\,kHz$, $U = 0.9\,U_{max}$, $I = I_N$, $\varphi_I = 0°$)

In Figure 6 the Fourier spectrum of a simulation approach and the analytical method without dead times are shown in a logarithmic scale so that the errors are visible. The simulation spectrum was evaluated using PLECS and its FFT function. The simulation approach shows a much higher error harmonics

between the carrier bands. This harmonics are caused by the window function [6] and mainly by the step size of the numerical solver. This effect leads to long simulation times and a high numerical error by simulating the inverter. The analytical method shows much lower error. An error is caused by numerical solving of the sine triangular modulation. Since the numerical solver has to calculate the points of intersection and not to solve a differential equation the precision is much more accurate. The calculation of the Fourier coefficients is limited in precision due to sin or cos evaluation and the data type. This error is also very low compared to solving the differential equations numerically.

The analytical method also requires significantly less computing time. While the analytical calculation in a MATLAB script takes about 30 seconds up to 3 minutes, the simulation and FFT in PLECS takes about 5 to 45 minutes. The required computing time for both methods increases with the ratio of f_S to f_1 and the maximum considered frequency of the FFT. In order to increase the accuracy of the simulation, the relative error of the solver must be reduced. This significantly increases the simulation time.

Dead time effects on harmonics

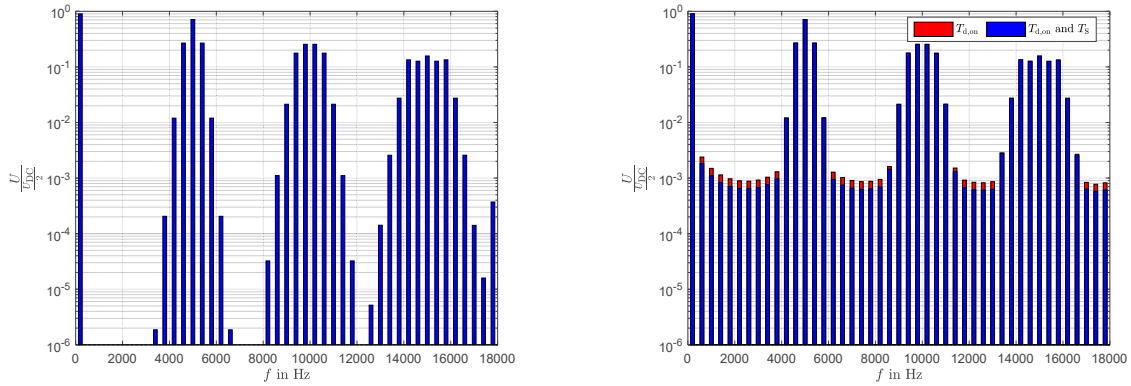

a) Reference without dead times

b) With dead times of Si IGBT module

Fig. 7: Fourier spectrum comparison without dead time, turn on delay and turn on delay with switching dead time ($f_1 = 200\,Hz$, $f_S = 5\,kHz$, $U = 0.9\,U_{max}$, $I = I_N$, $\varphi_I = 0°$)

In Figure 7 the Fourier spectrum without dead times, turn on delay as well ($T_{d,on}$) as turn on delay and switching times ($T_{d,on}$ and T_S) are shown. In case of no dead times the fundamental wave, the carrier and sideband harmonics are clearly identifiable. If switching dead times are taken into account, additional harmonics can be seen. Especially new harmonics will arise between the carrier bands. As already mentioned the additional harmonics are caused by voltage time area error.

In Figure 7b) comparison between the harmonics with turn on delay and turn on delay with switching behavior is shown. One can observe the harmonics in case of turn on delay and switching times the harmonics are lower then in case of only taking turn on delay into account.

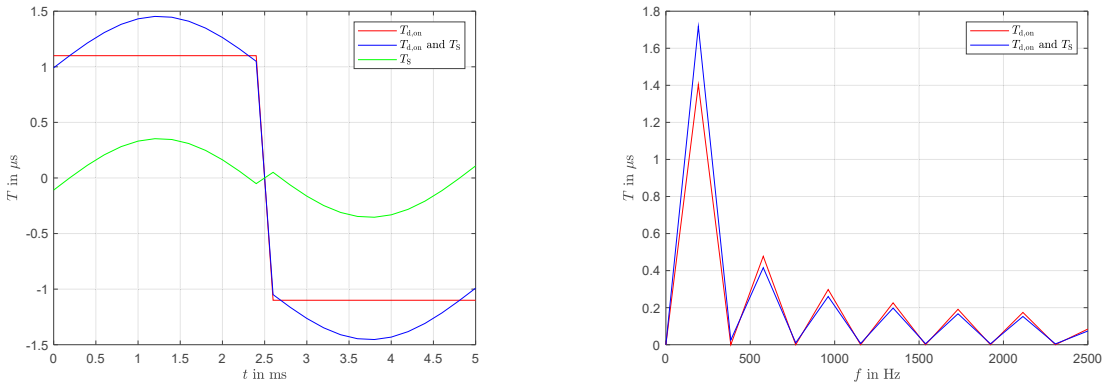

a) Dead time over fundamental wave

b) FFT of dead time

Fig. 8: Explanation for dead times effect ($f_1 = 200\,Hz$, $f_S = 5\,kHz$, $U = 0.9\,U_{max}$, $I = I_N$, $\varphi_I = 0°$)

In figure 8 the explanation for this effect is shown. On the left side the dead times are plotted over a fundamental wave. The case with turn on delay and switching times is more sinusoidal than the case with turn on delay. Applying a Fast Fourier Transformation (FFT) on the dead times, the effects on harmonics can be explained. The impact in case of turn on delay and an switching times on the fundamental harmonics is great and lower on the other harmonics than in case of only modeling the turn on delay. This could also be observed in the harmonics in 7b).

Comparision of Si IGBT and SiC MOSFET module

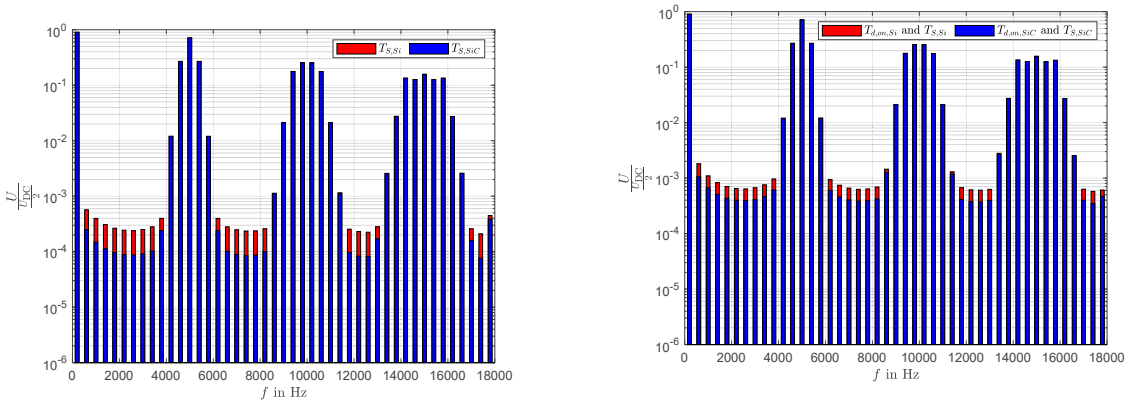

a) Harmonics with switching dead times

b) Harmonics with switching dead times and turn on delay

Fig. 9: Comparison of harmonics with Si IGBT and SiC MOSFET module ($f_1 = 200\,Hz$, $f_S = 5\,kHz$, $U = 0.9\,U_{max}$, $I = I_N$, $\varphi_I = 0°$)

In Figure 9a) the harmonics for the Si IGBT and the SiC MOSFET modules are compared. The additional harmonics caused by the switching dead times of the Si module are twice as high as for the SiC module. The higher current harmonics are caused by the higher switching dead time of the Si IGBT module as already presented in Figure 5.

Additionally when using the Si IGBT module the switching times are much higher. To prevent a short circuit of the Si module the turn on delay has to be higher as for the fast switching SiC module. This will also cause higher harmonics as shown in Figure 9b). For the Si IGBT module a turn on delay of 1.1 μs and 0.6 μs for the SiC MOSFET module is chosen. The harmonics caused by the turn on delay and switching times of the Si module are also about twice as high as with the SiC module.

Harmonic reduction of parallel rectifiers

For higher power two or more rectifiers have to be switched in parallel. In the following the reduction of harmonics with an appropriate control is presented. Two spectra with a phase offset can be superimposed using the following equation:

$$A_{\mathrm{k,res}} = A_{\mathrm{k}} \cos\left(\omega t - \varphi_{\mathrm{k},1}\right) + A_{\mathrm{k}} \cos\left(\omega t - \varphi_{\mathrm{k},2}\right) = 2A_{\mathrm{k}} \cos\left(\frac{\varphi_{\mathrm{k},1} - \varphi_{\mathrm{k},2}}{2}\right) \cos\left(\omega t - \frac{\varphi_{\mathrm{k},1} + \varphi_{\mathrm{k},2}}{2}\right) \quad (6)$$

The resulting amplitudes of the harmonics normalized to one rectifier can be calculated as follows:

$$|A_{\mathrm{k,res}}| = A_{\mathrm{k}} \left(\cos\frac{\varphi_{\mathrm{k},1} - \varphi_{\mathrm{k},2}}{2}\right) \quad (7)$$

Now the phase shift has to be determined. One possibility is the elimination of the carrier harmonics. The condition for the elimination is determined by the equation:

$$\varphi_2 = \varphi_1 + \frac{T_{\mathrm{S}}}{T_1} 180^\circ = \varphi_1 + \frac{f_1}{f_{\mathrm{S}}} 180^\circ \quad (8)$$

This condition has to be realized with a suitable control.

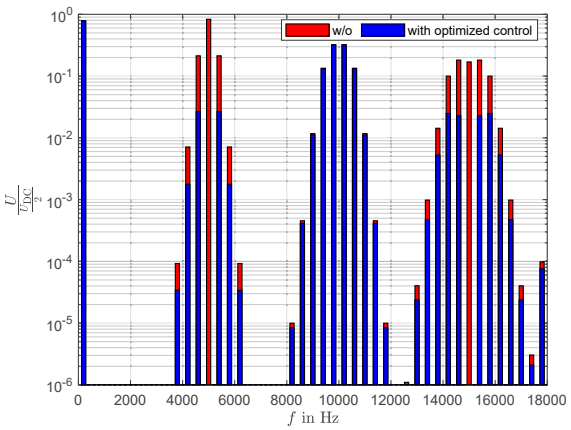

Fig. 10: Harmonic reduction with two parallel rectifiers ($f_1 = 200\,Hz$, $f_{\mathrm{S}} = 5\,kHz$, $U = 0.7\,U_{\mathrm{max}}$, $I = I_{\mathrm{N}}$, $\varphi_{\mathrm{I}} = 0^\circ$)

In figure 10 the harmonics without and with the optimized control are compared. It can be observed that the carrier harmonics in the first and third carrier band are eliminated. Also a reduction of the sideband harmonics can be seen.

Evaluation of interference current

Until now the voltage harmonics was considered. Now an easy approach for calculating the interference current will be presented. Since the harmonics caused by the inverter will be filtered out by the intermediate circuit capacitor, only harmonics caused by the rectifier will be taken into account.

The voltage harmonics can be calculated as presented. With the circuit of the transformer in Figure 1 one can calculate the current harmonics as follows:

$$|\underline{I}_{\mathrm{P,k}}| = \frac{|\underline{I}_{\mathrm{S,k}}|}{\ddot{u}} = \frac{|\underline{U}_{\mathrm{Rec,k}}|}{\ddot{u}\sqrt{(2\pi k f_1 L_\sigma)^2 + (R_\sigma)^2}} \quad (9)$$

To evaluate the influence of the interference current filter bands have to be determined. For this purpose the filter bands 4,75 - 6,25 kHz, 9,5 - 14,5 kHz and 14,51 - 16,5 kHz are chosen (based on the filter bands

in [7]).

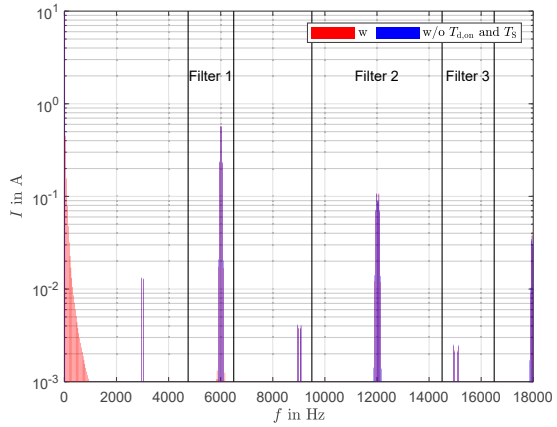

Fig. 11: Interference current ($f_1 = 16.7\,Hz$, $f_S = 3.006\,kHz$, $U = 0.7\,U_{max}$, $I = I_N$, $\varphi_I = 0°$)

In Figure 11 the spectrum of the interference current is shown. The harmonics are dominated by the carrier harmonics. The influence of dead times on the harmonics is small. Especially in the filter bands the influence is negligible and thus the filter values are nearly independent of the dead times.

Table II: Filter values for different switching frequencies ($f_1 = 16.7\,Hz$, $U = 0.7\,U_{max}$, $I = I_N$, $\varphi_I = 0°$)

f_S	Filter 1	Filter 2	Filter 3
1.002 kHz	260 mA	125 mA	35.8 mA
3.006 kHz	874 mA	219 mA	4.85 mA
5.010 kHz	6.50 mA	525 mA	2.82 mA
7.014 kHz	0.168 mA	376 mA	1.17 mA
9.018 kHz	0.369 mA	0.306 mA	0.624 mA

In table II the filter values for different switching frequencies are shown. For higher switching frequencies several harmonics can be reduced in the different filter bands. Since the limit value for the different filter bands are not equal a appropriate switching frequency has to be chosen. For 9 kHz the carrier harmonics are not inside any filter band and all values are below its limit.

The Si module has about 3.7 times higher switching losses than the SiC module. For the same switching losses a 3.7 higher switching frequency can be applied for the SiC module. This degree of freedom can be used to optimize the filter values and thus not to exceed the permissible limit.

Conclusion and outlook

In this paper an analytic method was presented to evaluate the harmonics caused by turn-on delay and switching dead times. It combines the possibility to model switching behavior as a function of the current and other parameters as well as small numerical error.

Effects caused by the dead times are shown and explained. An evaluation of the dead times and switching behavior on the interference current was presented.

Hence the influence of dead times on interference current is very small, using SiC with faster switching shows no direct benefit. Through lower switching losses with SiC higher frequencies are reachable. This enables a new degree of freedom in which the switching frequency can be chosen to optimize the filter values.

References

[1] D. G. Holmes and T. A. Lipo, “Pulse width modulation for power converters: Principles and practice”, vol. 2 of IEEE Press series on power engineering. Piscataway, NJ: IEEE Press, 2003

[2] S. Bernet, “Selbstgeführte Stromrichter am Gleichspannungszwischenkreis”. Berlin, Heidelberg: Springer Berlin Heidelberg, 2012

[3] T. W. Rasmussen, A. Vashishtha, and A. Jotwani, “Investigation of harmonics content in pwm natural and regular sampling including dead time and load current phase,” in 2020 22nd European Conference on Power Electronics and Applications (EPE’20 ECCE Europe), pp. P.1–P.10, IEEE, 92020

[4] M. Seilmeier, C. Wolz, and B. Piepenbreier, “Modelling and model based compensation of nonideal characteristics of two-level voltage source inverters for drive control application,” in 2011 1st International Electric Drives Production Conference, pp. 17–22, IEEE, 092011

[5] L. Papula, “Mathematische Formelsammlung für Ingenieure und Naturwissenschaftler”. Wiesbaden: Vieweg+Teubner, 2006

[6] T. Kuttner, “Praxiswissen Schwingungsmesstechnik”. Wiesbaden: Springer Fachmedien Wiesbaden, 2015

[7] “Technische Regelung für den Nachweis der elektromagnetischen Verträglichkeit zwischen Schienenfahrzeugen und der Infrastruktur im Geltungsbereich der EBO (TR-EMV) Teil 2 - Nachweis der Einhaltung der Störstromgrenzwerte”, https://www.eba.bund.de/SharedDocs/Downloads/DE/Fahrzeuge/Fahrzeugtechnik/EMV/31_Regelung_TR_EMV_Teil_2.pdf?__blob=publicationFile&v=7, 2015